Kinetic and Structural Investigations into the Allosteric and pH Effect on the Substrate Specificity of Human Epithelial 15-Lipoxygenase-2
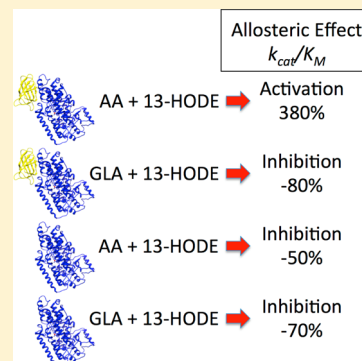
Netra Joshi,[†] Eric K. Hoobler,[†] Steven Perry,[†] Giovanni Diaz,[†] Brian Fox,[‡] and Theodore R. Holman*,[†]

[†]Department of Chemistry and Biochemistry, University of California, Santa Cruz, California 95064, United States
[‡]Center for Eukaryotic Structural Genomics and Department of Biochemistry, University of Wisconsin, Madison, Wisconsin 53706, United States

S *Supporting Information*

ABSTRACT: Lipoxygenases, important enzymes in inflammation, can regulate their substrate specificity by allosteric interactions with their own hydroperoxide products. In this work, addition of both 13-(S)-hydroxy-(9Z,11E)-octadecadienoic acid [13-(S)-HODE] and 13-(S)-hydroperoxy-(6Z,9Z,11E)-octadecatrienoic acid to human epithelial 15-lipoxygenase-2 (15-LOX-2) increases the k_{cat}/K_M substrate specificity ratio of arachidonic acid (AA) and γ-linolenic acid (GLA) by 4-fold. 13-(S)-HODE achieves this change by activating k_{cat}/K_M^{AA} but inhibiting k_{cat}/K_M^{GLA}, which indicates that the allosteric structural changes at the active site discriminate between the length and unsaturation differences of AA and GLA to achieve opposite kinetic effects. The substrate specificity ratio is further increased, 11-fold in total, with an increase in pH, suggesting mechanistic differences between the pH and allosteric effects. Interestingly, the loss of the PLAT domain affects substrate specificity but does not eliminate the allosteric properties of 15-LOX-2, indicating that the allosteric site is located in the catalytic domain. However, the removal of the PLAT domain does change the magnitude of the allosteric effect. These data suggest that the PLAT domain moderates the communication pathway between the allosteric and catalytic sites, thus affecting substrate specificity. These results are discussed in the context of protein dimerization and other structural changes.

Allosteric Effect k_{cat}/K_M	
AA + 13-HODE	Activation 380%
GLA + 13-HODE	Inhibition -80%
AA + 13-HODE	Inhibition -50%
GLA + 13-HODE	Inhibition -70%

Lipoxygenases (LOX) represent a class of non-heme iron-containing enzymes that catalyze the stereospecific peroxidation of polyunsaturated fatty acids (PUFAs) containing at least one 1,4-*cis*-pentadiene moiety.[1−4] There are three main types of human LOXs, 5-LOX, 12-LOX, and 15-LOX, that are named according to their positional specificity with arachidonic acid (AA).[5] The crystal structures of two mammalian LOXs indicate a single polypeptide chain folding into a two-domain structure.[6−8] The C-terminal catalytic domain consists of primarily α-helices and possesses the catalytic site, with the as-isolated non-heme ferrous ion, which is coordinated by water and endogenous ligands. The smaller N-terminal domain consists of primarily β-sheets and resembles the C2 domain of human lipases, known as PLAT domains (polycystin-1, lipoxygenase, α-toxin),[9] and has been implicated in membrane binding[10,11] and autoinactivation.[12,13]

Humans ingest and/or synthesize more than seven important fatty acids that are substrates to the six human LOX isozymes, as well as to cyclooxygenase (COX) and cytochrome P450.[14] This complex web of interactions translates into an extensive list of possible LOX/COX/P450 products in the body, of which only a fraction are fully understood from a biological perspective. The LOX endogenous products differ in the carbon chain length, the number and position of unsaturation points, and the degree of oxidation, depending on the fatty acid substrate and LOX isozyme. Many of these LOX products are biologically active compounds that not only mediate cellular

pathways directly but also act as precursors for potent chemical mediators, such as leukotrienes,[15,16] resolvins,[17] lipoxins,[18−22] and protectins.[17,18] Regulation of the production of these LOX products involves a variety of cellular mechanisms,[18] with allostery emerging as one of the more intriguing pathways, because of its effect on substrate specificity.[23,24]

Allostery is the means by which cells communicate the effects of the physical interactions of their machinery, such as proteins, nucleotides, and small molecules. Because allostery is fundamentally thermodynamic in nature, the communication across a particular protein can be mediated by both conformational and dynamic fluctuations.[25] Typically, an allosteric effector regulates the activity of an enzyme, as is the case with phosphofructokinase-1 (PFK-1), where ATP inhibits activity and AMP increases activity.[26−28] However, in a few cases, allostery can regulate substrate specificity. The most notable system is that of ribonucleotide reductase (RNR), which produces deoxynucleotides from ribonucleotides.[29−31] RNR must maintain proportional concentrations of the four deoxynucleotides in the cell and utilizes allostery to do this. RNR regulates its enzyme activity for a particular ribonucleotide by binding a deoxynucleotide, such as GDP or dTTP. The binding of the deoxynucleotide effector molecule to the

specificity site alters the structure of a shared loop with the catalytic site, thus altering RNR's substrate specificity from 2- to 10-fold.[31]

5-LOX was the first LOX isozyme to be shown to possess allostery,[32−35] with calcium and ATP activating its V_{max}/K_M by >25-fold.[35] The substrate specificity was also affected by calcium and ATP, with the V_{max}/K_M ratio of AA/EPA increasing 1.8-fold.[35] With respect to the human 15-LOXs, our laboratory first observed that the kinetic isotope effect of 15-LOX-1 increased with the addition of oleyl sulfate, suggesting a ternary complex and allostery.[36] It was then observed that LOX products changed the substrate specificity for both 15-LOX-1 and 15-LOX-2.[23,24] For 15-LOX-1, it was shown that 13-(S)-HODE, the product of 15-LOX with linoleic acid (LA), increased the $k_{cat}/K_M^{AA/LA}$ substrate specificity ratio.[23] 13-(S)-HODE also affected the kinetics of 15-LOX-2; however, the effect was more complicated. 13-(S)-HODE appeared to have a tighter affinity for 15-LOX-2 than for 15-LOX-1, and the allosteric effect was pH-dependent. It was observed that the pH increased the $k_{cat}/K_M^{AA/LA}$ substrate specificity ratio of 15-LOX-2, yielding a pH titration curve (pK_a of 7.7 ± 0.1), which suggested the possible involvement of a histidine residue.[23,24] On the basis of these data, homology modeling indicated that the possible location of the allosteric site could be between the catalytic domain and the PLAT domain, with His627 at the bottom of the cleft to interact with the carboxylic acid of 13-(S)-HPODE.[24] As mentioned above, the PLAT domain of LOX is important for membrane association, because removal of the PLAT domain from various LOX orthologues produced a decrease in liposome affinity.[12,13,37−39] The loss of the PLAT domain also lowered the activity for almost all the LOX isozymes investigated; however, the PLAT domain was not implicated in affecting substrate specificity. Given the pH dependency of 15-LOX-2's substrate specificity and the importance of allostery due to the availability of various LOX substrates in the cellular milieu, this work investigated the kinetic nature of 15-LOX-2's allostery and its pH dependence more thoroughly. In addition, the location of the allosteric site was further probed by removal of the PLAT domain, and its effects on the catalytic and allosteric response of 15-LOX-2 were probed.

■ MATERIALS AND METHODS

Materials. All the commercial fatty acids were purchased from Nu Chek Prep, Inc., and Sigma-Aldrich Chemical Co. The fatty acids were further repurified using a Higgins HAISIL (5 μm, 250 mm × 10 mm) C-18 column. An isocratic elution of 85% A (99.9% methanol and 0.1% acetic acid) and 15% B (99.9% water and 0.1% acetic acid) was used to purify all the fatty acids. Postpurification, the fatty acids were stored at −80 °C for a maximum of 6 months. Different lipoxygenase products were generated by reacting fatty acids with the appropriate LOX isozyme, such as 13-(S)-HPODE from soybean LOX-1 with LA and 13-(S)-HPOTrE (γ) from 15-LOX-2 with γ-linolenic acid (GLA). Briefly, the protocol involved reacting 50 μM substrate to completion with the enzyme in 500 mL of reaction buffer. A small sample from the large reaction was monitored on the UV spectrometer until complete turnover had been achieved. The products were then extracted using dichloromethane, reduced with trimethyl phosphite, evaporated to dryness, and reconstituted in methanol. The products were purified via high-performance liquid chromatography using an isocratic elution of 75% A

(99.9% methanol and 0.1% acetic acid) and 25% B (99.9% water and 0.1% acetic acid). The purities of the products were tested using liquid chromatography and tandem mass spectrometry and found to be >98%. All other chemicals were of high quality and used without further purification.

Overexpression and Purification of 15-LOX-2 and 15-LOX-2^{NoPLAT}. Purification of wild-type 15-LOX-2 (15-LOX-2) and the 15-LOX-2 PLAT domain truncation mutant (15-LOX-2^{NoPLAT}) was conducted using a construct encoding a fusion protein consisting of an N-terminal His$_8$ tag fused to maltose binding protein (MBP). The parent plasmid used in these studies, pVP68K, is available from the Protein Structure Initiative Materials Repository (http://www.psimr.asu.edu). The 15-LOX-2 fusion and the 15-LOX-2^{NoPLAT} fusion were expressed using the pVP68K-102188 and pVP68K-Ndelta188 plasmids, respectively, in *Escherichia coli* BL21(DE3), where the first 118 amino acids were removed for the truncated enzyme, 15-LOX-2^{NoPLAT}. For expression of the proteins, the host cells were grown to an OD of 0.6 at 37 °C, induced by decreasing the temperature to 20 °C, and grown overnight (16 h). The cells were harvested in 2 L fractions at a velocity of 5000g and then snap-frozen in liquid nitrogen. The cell pellets were resuspended in buffer A [25 mM Hepes (pH 8) and 150 mM NaCl] and lysed using a power laboratory press. The cellular lysate was centrifuged at 40000g for 25 min, and the supernatant was loaded onto an NTA-Ni affinity column. The column was washed with 15 mM imidazole in buffer A, followed by elution with 250 mM imidazole in buffer A (no NaCl). For 15-LOX-2, the fractions were collected, pooled together, and then dialyzed in 25 mM Hepes (pH 7.5) containing 150 mM NaCl, followed by overnight treatment with His$_6$-TEV protease at 4 °C. For 15-LOX-2^{NoPLAT}, the pooled fractions were dialyzed for 1 h against 25 mM Hepes (pH 7.5). It was then removed from the dialysis bag and cleaved with His$_6$-TEV protease for 1.5 h, followed by a second dialysis for 1 h in 25 mM Hepes (pH 6.5) containing 150 mM NaCl. The use of TEV protease was as previously described.[40] The proteolyzed 15-LOX-2 sample was applied to an NTA-Co^{2+} column and eluted in buffer A containing 15 mM imidazole. However, the proteolyzed 15-LOX-2^{NoPLAT} protein required a different procedure, which entailed an NTA-Ni^{2+} column and then an amylose column to bind residual MBP-tagged proteins. Both of these procedures were found to yield a >90% pure protein. It should be noted that after TEV cleavage, an unnatural serine is left on the N-terminus of both 15-LOX-2 proteins. The resulting nontagged 15-LOX-2 and 15-LOX-2^{NoPLAT} were concentrated by ultrafiltration (30 kDa molecular mass cutoff), combined with glycerol to yield a concentration of 20% (v/v), and then snap-frozen under liquid nitrogen. Overexpression and purification of soybean LOX-1 followed a protocol outlined previously.[41] The enzyme purity for all the isozymes was evaluated by sodium dodecyl sulfate−polyacrylamide gel electrophoresis (SDS−PAGE). The iron content of the LOX enzymes was determined with a Thermo Element XR inductively coupled plasma mass spectrometer (ICP-MS), using scandium (EDTA) or cobalt (EDTA) as an internal standard. Iron concentrations were compared to standard iron solutions. All the kinetic data were normalized to the iron content. The protein concentration was determined using the Bradford assay, with bovine serum albumin (BSA) as a protein standard. Briefly, Bradford protein dye reagent was diluted 1:5 using deionized water. Different solutions of BSA in deionized water were prepared, at concentrations ranging from 0 to 1 mg/mL

Table 1. Comparison of the Kinetic Parameters of 15-LOX-2 with Various Substrates at pH 7.5 and 8.5[a]

	k_{cat}/K_M (μM^{-1} s^{-1})		k_{cat} (s^{-1})	
	pH 7.5	pH 8.5	pH 7.5	pH 8.5
GLA	0.64 ± 0.02	0.37 ± 0.03	1.8 ± 0.03	1.1 ± 0.02
AA	0.40 ± 0.02	0.76 ± 0.06	1.5 ± 0.03	2.0 ± 0.04
DGLA	0.26 ± 0.04	0.49 ± 0.08	1.5 ± 0.08	1.8 ± 0.1
EPA	0.72 ± 0.03	1.4 ± 0.07	2.1 ± 0.02	2.8 ± 0.04
AA/GLA	0.63 ± 0.04	2.1 ± 0.03	0.83 ± 0.02	1.8 ± 0.05
AA/DGLA	1.5 ± 0.2	1.6 ± 0.3	0.99 ± 0.06	1.1 ± 0.07
AA/EPA	0.56 ± 0.04	0.54 ± 0.05	0.71 ± 0.02	0.72 ± 0.02

[a]Enzymatic assays were performed in 25 mM Hepes at 22 °C.

(linear range of the assay for BSA). Diluted Bradford reagent and BSA stocks were mixed in a 50:1 ratio, vortexed, and incubated for 5 min. Similarly, protein samples with diluted Bradford reagent were made in duplicate. All the samples were then spun down, and the absorbance was recorded at 595 nm on Perkin-Elmer Lambda 40 instrument. The concentration of the proteins was extrapolated from the standard curve of BSA.

Effect of pH Using the Competitive Substrate Capture Method. The competitive substrate capture method experiments were performed on the AA−LA substrate pair at pH 7.5 and 8.5 with 15-LOX-2 (from the SF9 and *E. coli* expression system) and 15-LOX-2[NoPLAT] using the previously described protocol.[23] Briefly, the AA−LA mixture was prepared with a molar ratio of 1:1. The reaction was initiated by adding (all normalized to Fe content) ∼20 nM 15-LOX-2 (*E. coli*), ∼50 nM 15-LOX-2 (SF9), and ∼90 nM 15-LOX-2[NoPLAT] to a 30 mL reaction cuvette [25 mM Hepes (pH 7.5 or 8.5)] at room temperature, with a total substrate concentration of 1 μM. The reaction was quenched at 5% substrate turnover using 1% glacial acetic acid. The reaction mixture was then extracted with DCM and evaporated to dryness under vacuum. The dried sample was reconstituted in 100 μL of methanol, centrifuged, and stored at −20 °C. The substrate capture ratio (k_{cat}/K_M) of AA and LA was determined from the peak areas and normalized on the basis of the ratio of the substrates present in the initial mixture.

Effect of pH on the Steady-State Substrate Specificity Kinetics. Lipoxygenase activity was assayed spectrophotometrically (Perkin-Elmer lambda 40) by monitoring an increase in absorbance at 234 nm due to formation of a conjugated diene product (ε = 25000 M^{-1} cm^{-1}). The reaction was conducted in 25 mM Hepes buffer (pH 7.5 or 8.5), at a constant ionic strength of 200 mM, at room temperature, in a final reaction volume of 2 mL, and at substrate concentrations ranging from 1 to 20 μM. Assays were initiated by adding 45−55 nM 15-LOX-2 and 100−200 nM 15-LOX-2[NoPLAT] (concentration normalized to iron content) and were constantly stirred using a magnetic stir bar. Assays for the different substrates were performed on the same day to allow a direct comparison and minimize error between AA and GLA data. The substrate concentrations were quantitatively determined by allowing the enzymatic reaction to go to completion. Initial rates were recorded at each substrate concentration and fit to the Michaelis−Menten equation using KaleidaGraph (Synergy) to determine k_{cat} and K_M values.

Effect of LOX Products on Steady-State Substrate Specificity Kinetics. GLA steady-state kinetics experiments were performed in the presence of two different lipoxygenase products, 13-(S)-HODE and 13-(S)-HOTrE(γ) at pH 7.5 and

8.5 with product concentrations of 0, 5, 15, and 30 μM. For the AA kinetics, initially the effect of both the products was tested with and without 15 μM 13-(S)-HODE and 13-(S)-HOTrE(γ) at both pH values. Further, the effect of 13-(S)-HODE on AA kinetics was investigated in detail at lower concentrations of 13-(S)-HODE of 0, 1, 3, and 5 μM at pH 7.5. Enzymatic assays were conducted using the same conditions mentioned above (25 mM Hepes, pH 7.5 or 8.5, a constant ionic strength of 200 mM, and room temperature). The enzyme was incubated with product first (15 s), to facilitate their interaction, followed by an initiation of the reaction via addition of the substrate. The plots of K_M and k_{cat}/K_M versus product concentration were fit to the hyperbolic inhibition equations (*vide infra*).

CD Half-Transition Temperature Measurements. Protein unfolding was monitored by CD measurements at 220 nm using an AVIV model 62DS CD spectrometer in a 0.1 cm quartz cuvette. Both 15-LOX-2 and 15-LOX-2[NoPLAT] samples (volume of 200 μL) consisted of 5 μM enzyme, 25 mM Hepes, and 150 mM NaCl (pH 7.5). Measurements were taken between 10 and 80 °C, at intervals of 5 °C, except close to T_{50}, where the intervals were decreased to 2 °C. Each temperature recording occurred after a 10 min equilibration period.

■ RESULTS AND DISCUSSION

Overexpression and Purification of 15-LOX-2 and 15-LOX-2[NoPLAT]. Methods developed for structural genomics studies of eukaryotic proteins were applied to the expression and purification of 15-LOX-2 and 15-LOX-2[NoPLAT].[42] After low-temperature growth for 16 h (20 °C) and no IPTG induction, approximately 40 mg of the His$_8$-MBP fusion protein per 2 L of medium was isolated, at approximately 80% purity after the first IMAC column. After cleavage of the His$_8$-MBP tag with TEV protease,[40] and subtractive IMAC, approximately 75% of the 15-LOX-2 and 15-LOX-2[NoPLAT] were recovered, giving a final yield of approximately 30 mg of pure protein per 2 L of culture medium. The final proteins isolated from *E. coli* were 90% pure as judged by SDS−PAGE, which was comparable to the purity previously achieved using the SF9 expression system.[43] However, ICP-MS data indicated that 15-LOX-2 and 15-LOX-2[NoPLAT] had iron contents ranging from 25 to 45%, which are greater than those of our previous SF9 15-LOX-2 preparations.[23,24,44] The steady-state kinetics of this *E. coli* preparation of 15-LOX-2 was also compared to that of the SF9 preparation and found to be significantly more active per active site iron (Table 1).[23] With AA as a substrate, the k_{cat} was 2-fold greater and the k_{cat}/K_M 4-fold greater than that of the SF9 preparation of 15-LOX-2.[23,24] Therefore, the unique benefits of this expression−purification method were its high yield in *E. coli*, its increased metal content, and its increased activity.
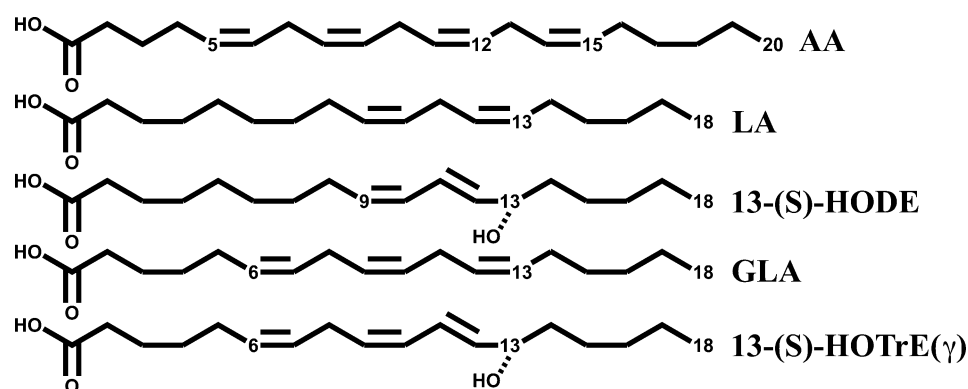
Figure 1. Structures of AA, LA, 13-(S)-HODE, GLA, and 13-(S)-HOTrE(γ).

Table 2. Comparison of Kinetic Parameters of 15-LOX-2 with AA and GLA, with and without Different C$_{18}$ Products (pH 7.5)[a]

	k_{cat}/K_M (μM^{-1} s^{-1})			k_{cat} (s^{-1})		
	AA	GLA	AA/GLA	AA	GLA	AA/GLA
no product	0.40 ± 0.02	0.64 ± 0.02	0.63 ± 0.04	1.5 ± 0.03	1.8 ± 0.03	0.83 ± 0.02
13-(S)-HODE	0.66 ± 0.07	0.29 ± 0.02	2.3 ± 0.3	1.3 ± 0.02	2.0 ± 0.06	0.65 ± 0.02
13-(S)-HOTrE(γ)	0.45 ± 0.03	0.32 ± 0.02	1.4 ± 0.01	1.4 ± 0.05	1.9 ± 0.04	0.73 ± 0.01

[a]Enzymatic assays were performed in 25 mM Hepes (pH 7.5) at 22 °C with and without 15 μM 13-(S)-HODE and 15 μM 13-(S)-HOTrE(γ).

Substrate Specificity Determined by Competitive Substrate Capture for 15-LOX-2. Our lab had previously reported a novel and simple method for determining the substrate specificity ratio of lipoxygenases.[23] Although k_{cat} and K_M cannot be determined for individual substrates via this method, it is still a very efficient method for comparing the k_{cat}/K_M ratios of different substrate pairs directly. To confirm that the newly E. coli-purified 15-LOX-2 behaves like the previously published SF9-purified 15-LOX-2, the substrate specificity ratio for AA to LA at pH 7.5 and 8.5 was determined using the competitive substrate capture method. The $k_{cat}/K_M^{AA/LA}$ ratio for E. coli 15-LOX-2 was found to be 2.3 ± 0.4 at pH 7.5 and 4.9 ± 0.5 at pH 8.5, which compare well with the $k_{cat}/K_M^{AA/LA}$ ratio values for SF9 15-LOX-2.[24] The results indicate that E. coli 15-LOX-2 shares substrate specificity under two pH conditions similar to that of SF9 15-LOX-2 and support the idea that they are similar enzymes.

Effect of pH on the Steady-State Substrate Specificity Kinetics of 15-LOX-2. To further investigate the pH effect on 15-LOX-2, steady-state kinetics were performed at different pH values on AA and GLA (Figure 1). While GLA is not found in the body at concentrations as high as those of LA, it was chosen for this investigation because it is a 20-fold better substrate than LA, which minimized error and allowed for more detailed allosteric kinetic analysis (vide infra). The kinetic data indicated that as the pH increased, GLA became a poorer substrate, with both k_{cat}^{GLA} and k_{cat}/K_M^{GLA} decreasing with increasing pH (Table 1). However, for AA both k_{cat}^{AA} and k_{cat}/K_M^{AA} increased with increasing pH. This pH effect resulted in a 3.4-fold increase in the $k_{cat}/K_M^{AA/GLA}$ ratio (0.63 ± 0.04 at pH 7.5 to 2.1 ± 0.03 at pH 8.5) and a 2.2-fold increase in the $k_{cat}^{AA/GLA}$ ratio (0.83 ± 0.02 at pH 7.5 to 1.8 ± 0.05 at pH 8.5). The other C$_{20}$ substrates, DGLA and EPA, also became better substrates with increasing pH, with EPA having an almost 2-fold greater k_{cat}/K_M than AA and an almost 3-fold greater k_{cat}/K_M than DGLA, correlating with their differences in unsaturation. It is unlikely that this difference in kinetic rates is due to formation of micelles because the critical micelle concentration of AA under

these conditions is 43 ± 3 μM as determined by isothermal titration calorimetry (MicroCal VP-ITC),[45] well above the concentrations used in these kinetic experiments. This showed that EPA and DGLA demonstrated a pH activation similar to that of AA (Table 1) and indicated a distinct catalytic mechanism for both substrate capture (k_{cat}/K_M) and product release (k_{cat}) between GLA and the other three C$_{20}$ fatty acid substrates. We are currently investigating the enzymatic mechanism of GLA with solvent isotope and viscosity effects to determine if its rate-limiting steps are comparable to those of AA.[46]

Effect of LOX Products on Steady-State Substrate Specificity Kinetics of 15-LOX-2. The allosteric effect of 13-(S)-HODE was previously demonstrated to affect the AA/LA ratio by competitive substrate capture methods,[23,24] but attempts to investigate the allosteric effect further proved to be difficult, because of the large error we encountered with LA as the substrate. With the discovery that GLA was a facile substrate and with the more active E. coli 15-LOX-2 preparation, the allosteric effects of 13-(S)-HODE and 13-(S)-HOTrE(γ) were investigated with steady-state kinetics on both AA and GLA, to more fully understand their allosteric properties (Table 2). It was observed that 13-(S)-HODE increased the k_{cat}/K_M^{AA} (from 0.40 ± 0.02 to 0.66 ± 0.07 μM^{-1} s^{-1}) but decreased the k_{cat}/K_M^{GLA} (from 0.64 ± 0.02 to 0.29 ± 0.02 μM^{-1} s^{-1}). 13-(S)-HOTrE(γ) exerted a similar effect by increasing the k_{cat}/K_M^{AA} and decreasing the k_{cat}/K_M^{GLA}, albeit to a lesser extent (Table 2). As a result, the addition of 13-(S)-HODE and 13-(S)-HOTrE(γ) elicited 3.7- and 2.2-fold increases in the $k_{cat}/K_M^{AA/GLA}$ ratio, respectively. These increases are comparable in direction and magnitude to the 3.3-fold pH effect on $k_{cat}/K_M^{AA/GLA}$, discussed above (Table 1). Interestingly, the $k_{cat}^{AA/GLA}$ ratio decreased slightly with the addition of 13-(S)-HODE (1.3-fold) and 13-(S)-HOTrE(γ) (1.1-fold), which was opposite to the pH effect, where the $k_{cat}^{AA/GLA}$ ratio increased by 2.2-fold (Table 1). These data represent clear similarities and distinctions between the

Table 3. Comparison of Kinetic Parameters of 15-LOX-2 with AA and GLA as Substrates and Different C$_{18}$ Products Added (pH 8.5)^a

	k_{cat}/K_M (μM^{-1} s^{-1})			k_{cat} (s^{-1})		
	AA	GLA	AA/GLA	AA	GLA	AA/GLA
no product	0.76 ± 0.06	0.37 ± 0.03	2.1 ± 0.2	2.0 ± 0.04	1.1 ± 0.02	1.8 ± 0.05
13-(S)-HODE	1.4 ± 0.1	0.21 ± 0.02	6.7 ± 0.8	1.9 ± 0.03	1.1 ± 0.02	1.7 ± 0.04
13-(S)-HOTrE(γ)	0.87 ± 0.09	0.22 ± 0.02	4.0 ± 0.5	1.8 ± 0.04	1.1 ± 0.03	1.6 ± 0.06

^{a}Enzymatic assays were performed in 25 mM Hepes (pH 8.5) at 22 °C with and without 15 μM 13-(S)-HODE and 15 μM 13-(S)-HOTrE(γ).

allosteric and pH effects with respect to k_{cat}/K_M (substrate capture) and k_{cat} (product release).

Combined Effects of the pH and Product on the Steady-State Substrate Specificity Kinetics of 15-LOX-2. The steady-state kinetic data presented above demonstrate that both pH (Table 1) and the two LOX products at pH 7.5 (Table 2) affected the kinetic parameters of GLA and AA. The ability of 13-(S)-HODE and 13-(S)-HOTrE(γ) to affect the kinetics was then investigated at pH 8.5, to determine if the pH and product effects were additive. As seen in Table 3, addition of 13-(S)-HODE and 13-(S)-HOTrE(γ) at pH 8.5 demonstrated the same trends in substrate specificity as at pH 7.5, with $k_{cat}/K_M^{AA/GLA}$ increasing and $k_{cat}^{AA/GLA}$ remaining unchanged. However, the magnitude of the AA/GLA substrate specificity ratios increased significantly, indicating that the pH and product effects were partially additive. For example, the $k_{cat}/K_M^{AA/GLA}$ substrate specificity ratio changed from 0.63 ± 0.04 at pH 7.5 with no product present (Table 2) to 6.7 ± 0.8 at pH 8.5 with 15 μM 13-(S)-HODE present (Table 3). This is an 11-fold increase in the substrate specificity ratio when both effects are taken into account and suggests the mechanisms of the pH and allosteric effects are similar but distinct.

Hyperbolic Inhibition of 15-LOX-2 by LOX Products. The overall trends for the 13-(S)-HODE and 13-(S)-HOTrE-(γ) effects were comparable; however, their magnitudes were different (Tables 2 and 3). These data suggested that the additional double bond at C$_6$ for 13-(S)-HOTrE(γ) (Figure 1) did register functional allosteric differences. This exquisite selectivity of the allosteric site between 13-(S)-HODE and 13-(S)-HOTrE(γ) is consistent with our previous data that demonstrated that 12-(S)-HETE and 15-(S)-HETE do not register any allosteric effect with 15-LOX-2.[23] Given this functional allosteric difference between 13-(S)-HODE and 13-(S)-HOTrE(γ), both products were titrated against 15-LOX-2, at pH 7.5 and 8.5 with GLA as the substrate. From the data, it was observed that 15-LOX-2 exhibited a hyperbolic response to increasing amounts of 13-(S)-HOTrE(γ) with an increase in K_M(app) for GLA from 2.8 to ~9.8 μM (Figure 2) and a decrease in k_{cat}/K_M(app) from 0.64 to ~0.28 μM^{-1} s^{-1} (Figure 3). The saturation behavior of K_M(app) and k_{cat}/K_M is indicative of hyperbolic inhibition (i.e., partial inhibition), as seen previously for soybean 15-LOX-1 and the inhibitor oleyl sulfate.[36] These data indicate the presence of an allosteric binding site that affects the catalysis by changing the microscopic rate constants of 15-LOX-2, as described in Scheme 1. From Scheme 1, eqs 1−4 allow for the determination of K_i, the strength of binding, α, the change in K_M, β, the change in k_{cat}, and β/α, the change in k_{cat}/K_M.

$$1/v = (\alpha K_M/k_{cat})[([I] + K_i)/(\beta[I] + \alpha K_i)] \times 1/[S]$$
$$+ 1/k_{cat} \times [([I] + \alpha K_i)/(\beta[I] + \alpha K_i)] \quad (1)$$

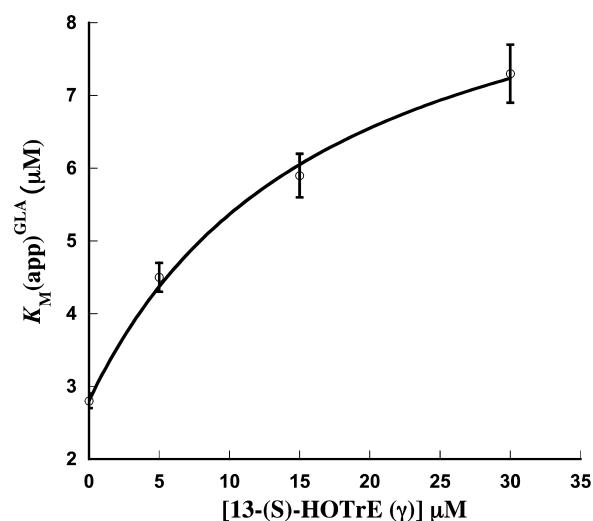**Figure 2.** Effect of 13-(S)-HOTrE(γ) on the K_M(app) of 15-LOX-2 with GLA (pH 7.5, 25 mM Hepes, 1−20 μM GLA at each product point). The data are fit to eq 2 (Scheme 1), where K_M = 2.8 μM. α and K_i were determined to be 3.5 ± 0.2 and 4.9 ± 0.7, respectively.
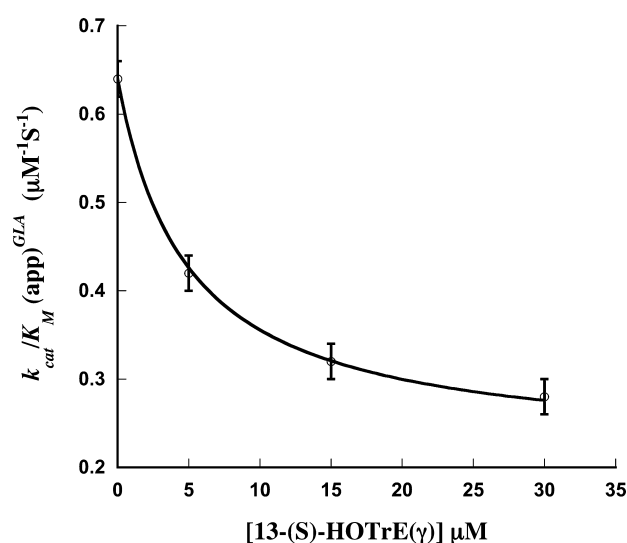

Figure 3. Effect of 13-(S)-HOTrE(γ) on the k_{cat}/K_M(app) of 15-LOX-2 with GLA (pH 7.5, 25 mM Hepes, 1−20 μM GLA at each product point). The data are fit to eq 3 (Scheme 1), where K_M = 2.8 μM, k_{cat} = 0.65 s^{-1}, α = 3.5, and K_i = 4.9 μM. β was determined to be 1.2 ± 0.02.

$$K_M(app) = \alpha K_M[([I] + K_i)/([I] + \alpha K_i)] \quad (2)$$

$$k_{cat}/K_M = (k_{cat}/\alpha K_M)[(\beta[I] + \alpha K_i)/([I] + K_i)] \quad (3)$$

$$k_{cat} = k_{cat}[(\beta[I] + \alpha K_i)/([I] + \alpha K_i)] \quad (4)$$

Scheme 1

$$E + S \underset{K_M}{\rightleftharpoons} E{\cdot}S \xrightarrow{k_2} E + P$$

A plot of K_M(app) with the addition of 13-(S)-HOTrE(γ) at pH 7.5 (Figure 2), when fitted with eq 2, yielded an α of 3.5 ± 0.2 and a K_i of 4.9 ± 0.7 μM. The values of α and K_i were then utilized in eq 3 and fit to the k_{cat}/K_M data (Figure 3), which yielded a β of 1.2 ± 0.02. The value of β was also determined from the k_{cat} data with eq 4, with the values of α and K_i given above applied (data not shown), which yielded a β of 1.2 ± 0.05 that matched well with the β value from the k_{cat}/K_M plot. These values indicate that the kinetics show mixed hyperbolic allostery, $\alpha > 1$ (K-type inhibition) and $\beta > 1$ (V-type activation),[47] with the majority of the kinetic change being seen in the value of K_M ($\alpha = 3.5 ± 0.2$) and only a slight effect on the k_{cat} ($\beta = 1.2 ± 0.02$). This comparison is best observed in the β/α value, the allosteric effect on k_{cat}/K_M, which is less than 1 ($\beta/\alpha = 0.34$) and indicates k_{cat}/K_M allosteric inhibition. The hyperbolic data suggest the formation of a catalytically active ternary complex (I·E·S) between 15-LOX-2 and 13-(S)-HOTrE(γ) and are consistent with our previous finding of an allosteric site in 15-LOX-2.[24] Similarly, graphing of steady-state kinetic data of 15-LOX-2 with 13-(S)-HOTrE(γ) at pH 8.5 gave an α of 2.0 ± 0.1 and a K_i of 6.1 ± 1 from the K_M plot (Supporting Information, Figure S1) and a β of 0.9 ± 0.04 from the k_{cat}/K_M (Supporting Information, Figure S2). From these data, it was observed that while the α and β values have decreased with pH, the K_i value for 13-(S)-HOTrE(γ) showed little pH dependence. Therefore, the pH change of the AA/GLA substrate specificity ratio was not due to a change in the affinity of 13-(S)-HOTrE(γ) at higher pH values, but more likely a pH-dependent structural change, which affected the allosteric communication between the catalytic and allosteric sites (α and β), but not 13-(S)-HOTrE(γ) binding.

Fitting the 13-(S)-HODE data in a similar manner yielded an α value of 7.3 ± 0.06 (K-type inhibition) and a K_i value of 9.8 ± 0.2 μM from the K_M(app) plot (Figure 4). The α value was double that of the α value for 13-(S)-HOTrE(γ), while the K_i value was comparable to that of 13-(S)-HOTrE(γ), indicative of a stronger allosteric effect on K_M for 13-(S)-HODE. This is supported by the lower β/α value of 0.22 for 13-(S)-HODE, compared to that of 13-(S)-HOTrE(γ) ($\beta/\alpha = 0.34$). The β value was determined to be 1.6 ± 0.1 (Figure 5), which is V-type activation, similar to that seen for 13-(S)-HOTrE(γ), and highlights a key similarity between the two LOX products. The 13-(S)-HODE data at pH 8.5 could not be fit using hyperbolic inhibition (Scheme 1) or a simple noncompetitive model; therefore, the change in k_{cat}/K_M(app) was plotted versus 13-(S)-HODE concentration and fit with a saturation curve (Supporting Information, Figure S3). Using this method, the K_D at pH 8.5 increased to 53 ± 25 μM, considerably greater than that observed at pH 7.5 (8.6 ± 0.7 μM), indicating a lower binding affinity with increasing pH. This lower affinity could account for the smaller change in k_{cat}/K_M^{GLA} with 13-(S)-

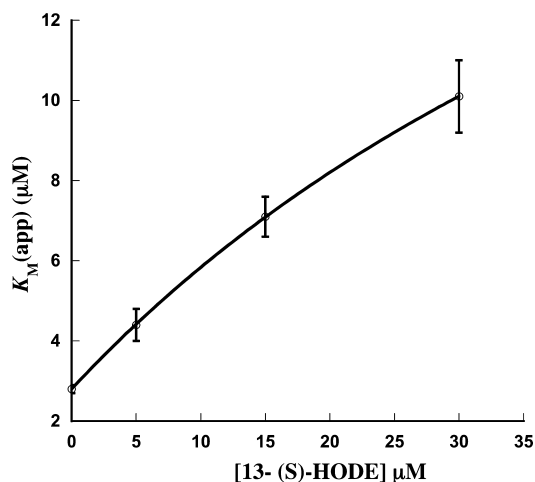**Figure 4.** Effect of 13-(S)-HODE on the K_M(app) of 15-LOX-2 with GLA (pH 7.5, 25 mM Hepes, 1–20 μM GLA at each product point). The data are fit to eq 2 (Scheme 1), where K_M = 2.8 μM. α and K_i were determined to be 7.3 ± 0.06 and 9.8 ± 0.2, respectively.
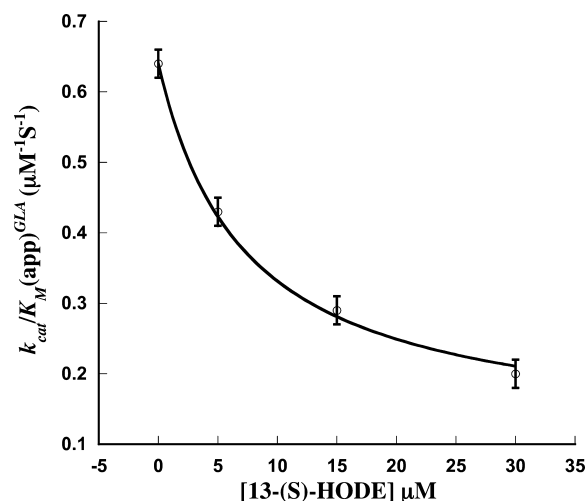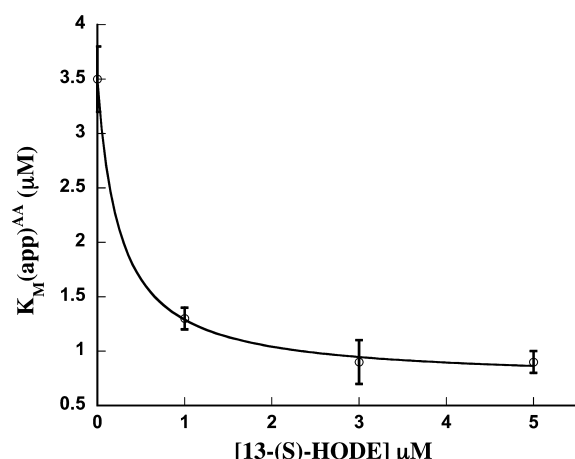

Figure 5. Effect of 13-(S)-HODE on the k_{cat}/K_M(app) of 15-LOX-2 with GLA (pH 7.5, 25 mM Hepes, 1–20 μM GLA at each product point). The data are fit to eq 3 (Scheme 1), where K_M = 2.8 μM, k_{cat} = 0.65 s^{-1}, α = 7.3, and K_i = 9.8 μM. β was determined to be 1.6 ± 0.1.

HODE at pH 8.5 than at pH 7.5 and not necessarily a change in α and β, although we cannot determine this directly. It should be noted that this alternative fitting method yielded a K_D of 8.6 ± 0.7 μM at pH 7.5 for 13-(S)-HODE, which was comparable to the K_i of 9.8 ± 0.2 μM found by the hyperbolic inhibition fit and validated this fitting method. Interestingly, the fact that 13-(S)-HODE binding was affected by pH but the binding of 13-(S)-HOTrE(γ) suggests that the structural differences between the two LOX products (i.e., degree of unsaturation) change their allosteric binding modes.

As described above, the addition of 15 μM 13-(S)-HODE and 13-(S)-HOTrE(γ) exhibited the opposite effects depending on the substrate, with the AA kinetics being activated and the GLA kinetics inhibited (Table 2). To investigate this effect further, titration kinetics with 13-(S)-HODE, the more potent activator, were determined with AA at pH 7.5. It was observed that 13-(S)-HODE affected AA kinetics with an α value of 0.2 ± 0.01 (K-type activation), a β value of 0.76 ± 0.01 (V-type inhibition), a β/α value of 3.8 (k_{cat}/K_M allosteric activation),

Figure 6. Effect of 13-(S)-HODE onthe K_M(app) of 15-LOX-2 with AA (pH 7.5, 25 mM Hepes, 1−20 μM AA at each product point). The data are fit to eq 2 (Scheme 1), where K_M = 3.5 μM. α and K_i were determined to be 0.2 ± 0.01 and 1.2 ± 0.03, respectively.
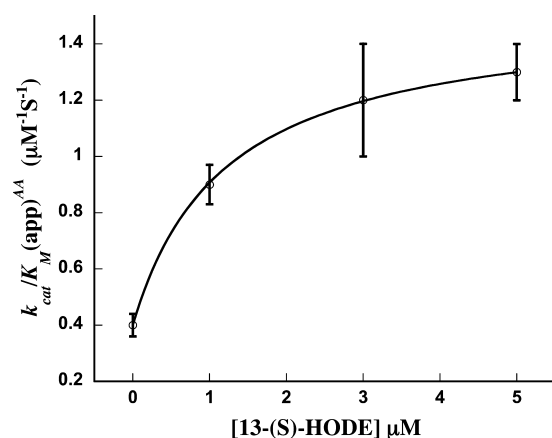

Figure 7. Effect of 13-(S)-HODE on the k_{cat}/K_M(app) of 15-LOX-2 with AA (pH 7.5, 25 mM Hepes, 1−20 μM AA at each product point). The data are fit to eq 3 (Scheme 1), where K_M = 3.5 μM, k_{cat} =1.4 s^{-1}, α = 0.2, and K_i = 1.2 μM. β was determined to be 0.76 ± 0.01.

and a K_i value of 1.2 ± 0.03 μM (Figures 6 and 7). The β/α values with 13-(S)-HODE/AA is the opposite of that seen with 13-(S)-HODE/GLA, which showed k_{cat}/K_M allosteric inhibition (β/α = 0.22). In addition, the β value for 13-(S)-HODE/AA indicated V-type inhibition, which was the opposite of the β value for 13-(S)-HODE/GLA (V-type activation; β = 1.6 ± 0.1). This difference is significant because 13-(S)-HODE both activates and inhibits, depending on the length and unsaturation of the substrate, and suggests subtle structural changes in the active site. It should be noted that we previously reported a slight inhibition of both k_{cat} and k_{cat}/K_M at the single concentration of 10 μM 13-(S)-HPODE and AA.[23] We were not able to reproduce this result, and considering that the previous data utilized only one product concentration and one pH condition, we consider the current data more reliable for interpretation. In addition, 13-(S)-HODE manifested different thresholds of response, with the allosteric effect on AA catalysis occurring at a lower concentrations than the allosteric effect on GLA catalysis (K_i values of 1.2 ± 0.03 and 9.8 ± 0.02 μM, respectively). These differences in K_i values are difficult to rationalize with the current one-site allosteric model. The data may indicate two distinct allosteric sites with distinct K_i values

or two distinct 15-LOX-2 species, which bind 13-(S)-HODE with different affinities, such as E·AA and E·GLA. Further studies are required to differentiate these possible explanations. Finally, the K_i for 13-(S)-HODE binding with AA as the substrate is considerably greater than was estimated by our competitive substrate capture method with both AA and LA being present.[24] Considering that the K_i for 13-HODE varies with AA and GLA, it could be possible that the presence of LA also affects the K_i value of 13-(S)-HODE, which we are currently investigating further.

Summary of 15-LOX-2 Data. In summary, the wild-type 15-LOX-2 kinetic results showed that GLA and AA had different responses to pH, indicating that the molecular mechanisms for GLA and AA were distinct. Addition of 13-(S)-HODE and 13-(S)-HOTrE(γ) mirrored the k_{cat}/K_M pH effect, with an increase in $k_{cat}/K_M^{AA/GLA}$; however, the pH and allosteric effects were additive, with the combined effect being 11-fold, suggesting both mechanistic similarities and differences between the pH and allosteric effects. The two allosteric effectors, 13-(S)-HODE and 13-(S)-HOTrE(γ), displayed comparable hyperbolic inhibition kinetics; however, the K_i of 13-(S)-HODE was pH-dependent, while that of 13-(S)-HOTrE(γ) was not, indicating a difference in their binding modes and supporting the presence of a specific binding site, because it is unlikely their structural differences would affect nonspecific binding. Finally, it was observed that 13-(S)-HODE activated k_{cat}/K_M^{AA} but inhibited k_{cat}/K_M^{GLA}. This difference is significant and indicates that the allosteric structural changes differentiate the length and unsaturation of AA and GLA. Recently, it has been postulated that addition of 13-(S)-HODE induces dimer formation for rabbit 15-LOX-1 (i.e., 12/15-LOX);[48,49] however, the data presented above suggest a more complicated scenario. Considering the opposite effects of 13-(S)-HODE on GLA and AA catalysis, it is unlikely that only dimer formation could account for these two opposing effects (*vide infra*).

Characterization of the PLAT Domain Deletion Mutant (15-LOX-2^{NoPLAT}). *Thermal Stability Measurements of 15-LOX-2^{NoPLAT}.* Homology modeling of 15-LOX-2 previously suggested that its allosteric site could be located in a cleft between the PLAT and catalytic domains.[24] This hypothesis was investigated by removing the PLAT domain and generating 15-LOX-2^{NoPLAT}. The thermal stability of 15-LOX-2^{NoPLAT} was measured, and as seen in Figure 8, both 15-LOX-2 and 15-LOX-2^{NoPLAT} underwent a loss of secondary structure with a two-state unfolding transition and a T_{50} between 40 and 45 °C for both proteins. These data indicated the thermal stability of the truncated protein to be approximately the same as that of the wild-type protein.

Characterization of Steady-State Kinetics of 15-LOX-2^{NoPLAT} with AA and GLA. Steady-state kinetics were conducted with 15-LOX-2^{NoPLAT} at pH 7.5, using both AA and GLA to investigate the effect of removing the PLAT domain (Table 4). A loss of activity was observed for 15-LOX-2^{NoPLAT} with a 50% decrease in k_{cat}^{AA} (0.75 ± 0.03 s^{-1}) and was consistent with previous results, where an 84% decrease in k_{cat}^{AA} for rabbit 15-LOX-1^{NoPLAT} was observed.[13] The k_{cat}/K_M value of 15-LOX-2^{NoPLAT} also decreased approximately 50% (0.21 ± 0.02 μM^{-1} s^{-1}), which was also consistent with the previous 73% decrease in k_{cat}/K_M^{AA} for rabbit 15-LOX-1^{NoPLAT}.[13] In comparing the substrate specificity of 15-LOX-2^{NoPLAT} with AA and GLA, we observed that the $k_{cat}^{AA/GLA}$ ratio (0.76 ± 0.06) did not change much relative to that of 15-LOX-2 (0.83 ± 0.03). However, the
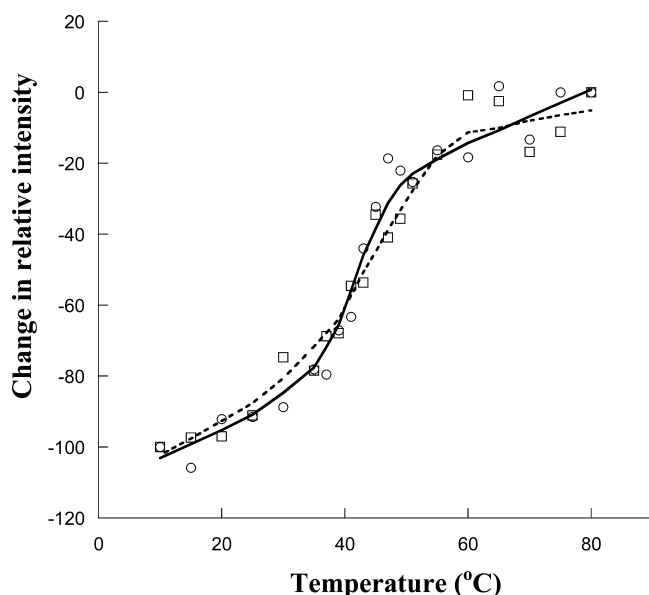
Figure 8. CD half-transition temperature (T_{50}) measurement for 15-LOX-2 (○) and 15-LOX-2^{NoPLAT} (□). The experiment was performed in 25 mM Hepes buffer [150 mM NaCl (pH 7.5)] between 10 and 80 °C.

$k_{cat}/K_M^{AA/GLA}$ ratio did change, with a ratio of 1.3 ± 0.2 for 15-LOX-2^{NoPLAT} and a ratio of 0.62 ± 0.04 for 15-LOX-2. These data indicated that the PLAT domain affected substrate specificity and warranted further investigation.

Substrate Specificity pH Profile of 15-LOX-2^{NoPLAT}. The competitive substrate capture method was employed to explore whether the PLAT domain was responsible for the pH effect on substrate specificity. It was determined that the $k_{cat}/K_M^{AA/GLA}$ ratio for 15-LOX-2^{NoPLAT} was found to be 2.5 ± 0.2 at pH 7.5 and 3.6 ± 0.3 at pH 8.5. These values were comparable to that found in this work for wild-type 15-LOX-2 (*vide supra*) and indicated that the PLAT domain had a minimal contribution to the pH effect.

Effect of 13-(S)-HODE on GLA and AA Steady-State Kinetics of 15-LOX-2^{NoPLAT}. Wild-type 15-LOX-2 demonstrated a hyperbolic allosteric effect, with 13-(S)-HODE and GLA (pH 7.5) (Table 5). For 15-LOX-2^{NoPLAT}, increasing amounts of 13-(S)-HODE also evoked a hyperbolic allosteric effect with GLA, revealing an α value of 4.9 ± 2, a β value of 1.6 ± 0.2, a β/α value of 0.33, and a K_i value of 6.1 ± 2 μM (Table 5 and Supporting Information, Figures S4 and S5). The fact that 15-LOX-2^{NoPLAT} had an allosteric response similar to that of 15-LOX-2 indicates that removal of the PLAT domain does not eliminate allostery and that the allosteric site is located in the catalytic domain.

The addition of 13-(S)-HODE to 15-LOX-2^{NoPLAT} with AA as a substrate, however, evoked kinetic behavior dramatically different from that of 15-LOX-2. The K_M(app) fit revealed an α

value of 2.3 ± 0.4, a β value of 1.1 ± 0.03, a β/α value of 0.48, and a K_i value of 2.0 ± 0.6 μM (Table 5 and Supporting Information, Figures S6 and S7). The fact that the β/α value is now 0.48, which is the opposite effect seen for 15-LOX-2 (β/α = 4), represents a significant change in the allosteric effect with removal of the PLAT domain. It should be noted that 13-(S)-HODE also manifests different K_i values for AA and GLA catalysis with 15-LOX-2^{NoPLAT}, similar to that seen for 15-LOX-2. These data support the hypothesis postulated above, that there are either two distinct allosteric sites or two distinct allosteric binding species, such as E·AA and E·GLA. Both of these hypotheses are being investigated further.

Summary of 15-LOX-2^{NoPLAT} Data. In summary, removal of the PLAT domain does not affect the overall protein stability and does not affect its kinetic pH dependence, indicating the source of the pH effect is in the catalytic domain and not at the interface of the two domains with H627, as postulated previously.[46] Alignments of the actives sites of 15-LOX-2 and 15-LOX-1[7] do not indicate a potential histidine in the 15-LOX-2 active site, as the pH dependence suggests;[46] however, it does not exclude the possibility of a buried histidine emerging into the active site upon catalytic protein motions. However, the removal of the PLAT domain did manifest a 2-fold increase in $k_{cat}/K_M^{AA/GLA}$, indicating that the PLAT domain does influence substrate specificity. Interestingly, 15-LOX-2^{NoPLAT} retained its allosteric properties, indicating that the allosteric site is also located in the catalytic domain, like the pH effect, and not in the cleft between the two domains. Nonetheless, removal of the PLAT domain does affect the degree of allostery (i.e., the sign and magnitude of α and β), suggesting that the PLAT domain does moderate the communication pathway between the allosteric and catalytic sites. Therefore, the PLAT domain has a role in not only membrane affinity[13] but also allostery and substrate specificity. Nonetheless, it is still unclear what specific biophysical changes occur upon allosteric effector binding. As mentioned above, Kuhn and co-workers proposed that dimerization was induced upon addition of 13-(S)-HODE to rabbit 15-LOX-1, and that the postulated dimerization interface was opposite to the PLAT domain, which is consistent with our current results. However, the SAXS data could not determine if dimerization was the only structural change.[48,49] It could be that the allosteric effect is responsible for not only dimerization but also specific structural changes in the active site, as seen in RNR,[29] or for protein dynamic changes, as seen for calbindin D$_{9k}$.[50] A possible explanation could be similar to that seen for COX-2. COX-2 is a homodimer, but binding of an inhibitor to only one of the monomers establishes a conformational heterodimer, whose active monomer has altered kinetic behavior.[51] 15-LOX-2 could also manifest a similar behavior where allosteric effectors not only induce dimerization but also bind to only one of the subunits, establishing a functional heterodimer. Continued efforts are underway to refine our understanding of the allosteric properties of 15-LOX-2 in terms of the location of the allosteric site and its molecular

Table 4. Comparison of Kinetic Parameters of 15-LOX-2 and 15-LOX-2^{NoPLAT}, with AA and GLA as Substrates (pH 7.5)^a

	k_{cat}/K_M (μM^{-1} s^{-1})			k_{cat} (s^{-1})		
	AA	GLA	AA/GLA	AA	GLA	AA/GLA
15-LOX-2	0.40 ± 0.02	0.64 ± 0.02	0.62 ± 0.04	1.5 ± 0.03	1.8 ± 0.03	0.83 ± 0.03
15-LOX-2^{NoPLAT}	0.21 ± 0.02	0.16 ± 0.02	1.3 ± 0.2	0.75 ± 0.03	0.99 ± 0.04	0.76 ± 0.06

^{a}Enzymatic assays were performed in 25 mM Hepes (pH 7.5) at 22 °C.

Table 5. Comparison of Hyperbolic Fit Parameters of 15-LOX-2 and 15-LOX-2$^{\text{NoPLAT}}$ with 13-(S)-HODE and AA or GLA as Substrates at pH 7.5^a

conditions	15-LOX-2				15-LOX-2$^{\text{NoPLAT}}$			
	K_i	α	β	β/α	K_i	α	β	β/α
GLA with 13-(S)-HODE	9.8 ± 0.2	7.3 ± 0.06	1.6 ± 0.1	0.22	6.1 ± 2	4.9 ± 2	1.6 ± 0.2	0.33
AA with 13-(S)-ODE	1.2 ± 0.03	0.2 ± 0.01	0.76 ± 0.01	3.8	2.0 ± 0.6	2.3 ± 0.4	1.1 ± 0.03	0.48

^{a}Enzymatic assays were performed in 25 mM Hepes (pH 7.5) at 22 °C with and without products.

mechanism. Synthetic allosteric effectors are also being investigated in the hopes of developing the allosteric site as a possible therapeutic target for LOX regulation by changing the proportions of LOX products produced, as opposed to inhibition of the entire enzymatic activity. If achieved, this could be an important advance, because some LOX products are beneficial while others are detrimental to human health.[17]

ASSOCIATED CONTENT

Supporting Information
Additional kinetic graphics. This material is available free of charge via the Internet at http://pubs.acs.org.

AUTHOR INFORMATION

Corresponding Author
*E-mail: tholman@chemistry.ucsc.edu. Phone: (831) 459-5884. Fax: (831) 459-2935.

Author Contributions
N.J. and E.K.H. contributed equally to this work.

Notes
The authors declare no competing financial interest.

ABBREVIATIONS

LOX, lipoxygenase; 15-LOX-2, human epithelial 15-lipoxygenase-2; 15-LOX-2$^{\text{NoPLAT}}$, human epithelial 15-lipoxygenase-2 with the PLAT domain removed; 15-LOX-1, human reticulocyte 15-lipoxygenase-1; rabbit 15-LOX, rabbit 15-lipoxygenase; 12-LOX, human platelet 12-lipoxygenase; soybean LOX-1, soybean lipoxygenase 1; 5-LOX, human 5-lipoxygenase; COX, cyclooxygenase; P450, cytochrome P450; TEV protease, tobacco etch virus protease; BSA, bovine serum albumin; MBP, maltose binding protein; NTA, nitrilotriacetic acid; IMAC, immobilized metal affinity chromatography; T_{50}, half-transition temperature; DCM, dichloromethane; AA, arachidonic acid; LA, linoleic acid; 13-(S)-HPODE, 13-(S)-hydroperoxy-(9Z,11E)-octadecadienoic acid; 13-(S)-HODE, 13-(S)-hydroxy-(9Z,11E)-octadecadienoic acid; GLA, (γ)-linolenic acid; 13-(S)-HPOTrE(γ), 13-(S)-hydroperoxy-(6Z,9Z,11E)-octadecatrienoic acid; 13-(S)-HOTrE(γ), 13-(S)-hydroxy-(6Z,9Z,11E)-octadecatrienoic acid; 9-(S)-HOTrE(γ), 9-(S)-hydroxy-(6Z,9Z,11E)-octadecatrienoic acid; DGLA, di-homo (γ) linolenic acid; EPA, eicosapentaenoic acid; k_{cat}, rate constant for product release; k_{cat}/K_M, rate constant for fatty acid capture; K_D, equilibrium constant for the dissociation of a ligand from the protein site; $k_{\text{cat}}/K_M[O_2]$, rate constant for O_2 capture.

REFERENCES

(1) Ivanov, I., Heydeck, D., Hofheinz, K., Roffeis, J., O'Donnell, V. B., Kuhn, H., and Walther, M. (2010) Molecular enzymology of lipoxygenases. *Arch. Biochem. Biophys. 503*, 161−174.

(2) Brash, A. R. (1999) Lipoxygenases: Occurrence, Functions, Catalysis and Acquisition of Substrate. *J. Biol. Chem. 274*, 23679−23682.

(3) Noguchi, N., Yamashita, H., Hamahara, J., Nakamura, A., Kuhn, H., and Niki, E. (2002) The specificity of lipoxygenase-catalyzed lipid peroxidation and the effects of radical-scavenging antioxidants. *Biol. Chem. 383*, 619−626.

(4) Schneider, C., Pratt, D. A., Porter, N. A., and Brash, A. R. (2007) Control of oxygenation in lipoxygenase and cyclooxygenase catalysis. *Chem. Biol. 14*, 473−488.

(5) Yamamoto, S. (1992) Mammalian lipoxygenases: Molecular structures and functions. *Biochim. Biophys. Acta 1128*, 117−131.

(6) Gilbert, N. C., Bartlett, S. G., Waight, M. T., Neau, D. B., Boeglin, W. E., Brash, A. R., and Newcomer, M. E. (2011) The structure of human 5-lipoxygenase. *Science 331*, 217−219.

(7) Choi, J., Chon, J. K., Kim, S., and Shin, W. (2008) Conformational flexibility in mammalian 15S-lipoxygenase: Reinterpretation of the crystallographic data. *Proteins 70*, 1023−1032.

(8) Gillmor, S. A., Villasenor, A., Fletterick, R., Sigal, E., and Browner, M. (1997) The structure of mammalian 15-lipoxygenase reveals similarity to the lipases and the determinants of substrate specificity. *Nat. Struct. Biol. 4*, 1003−1009.

(9) Chahinian, H., Sias, B., and Carriere, F. (2000) The C-terminal domain of pancreatic lipase: Functional and structural analogies with c2 domains. *Curr. Protein Pept. Sci. 1*, 91−103.

(10) May, C., Hohne, M., Gnau, P., Schwennesen, K., and Kindl, H. (2000) The N-terminal β-barrel structure of lipid body lipoxygenase mediates its binding to liposomes and lipid bodies. *Eur. J. Biochem. 267*, 1100−1109.

(11) Tatulian, S. A., Steczko, J., and Minor, W. (1998) Uncovering a calcium-regulated membrane-binding mechanism for soybean lipoxygenase-1. *Biochemistry 37*, 15481−15490.

(12) Walther, M., Hofheinz, K., Vogel, R., Roffeis, J., and Kühn, H. (2011) The N-terminal β-barrel domain of mammalian lipoxygenases including mouse 5-lipoxygenase is not essential for catalytic activity and membrane binding but exhibits regulatory functions. *Arch. Biochem. Biophys. 516*, 1−9.

(13) Walther, M., Anton, M., Wiedmann, M., Fletterick, R., and Kuhn, H. (2002) The N-terminal domain of the reticulocyte-type 15-lipoxygenase is not essential for enzymatic activity but contains determinants for membrane binding. *J. Biol. Chem. 277*, 27360−27366.

(14) Rouzer, C. A., and Marnett, L. J. (2011) Endocannabinoid oxygenation by cyclooxygenases, lipoxygenases, and cytochromes P450: Cross-talk between the eicosanoid and endocannabinoid signaling pathways. *Chem. Rev. 111*, 5899−5921.

(15) Samuelsson, B. (1983) Leukotrienes: Mediators of Immediate Hypersensitivity Reactions and Inflammation. *Science 220*, 568−575.

(16) Jampilek, J., Dolezal, M., Opletalova, V., and Hartl, J. (2006) 5-Lipoxygenase, leukotrienes biosynthesis and potential antileukotrienic agents. *Curr. Med. Chem. 13*, 117−129.

(17) Serhan, C., and Petasis, N. (2011) Resolvins and Protectins in Inflammation Resolution. *Chem. Rev. 111*, 5922−5943.

(18) Serhan, C. N., Chiang, N., and Van Dyke, T. E. (2008) Resolving inflammation: Dual anti-inflammatory and pro-resolution lipid mediators. *Nat. Rev. Immunol. 8*, 349−361.

(19) Kuhn, H., Brash, A. R., Wiesner, R., and Alder, L. (1988) Lipoxygenase catalyzed oxygenation of hydroxy fatty acids to lipoxins. *Adv. Exp. Med. Biol. 229*, 39−49.

(20) Samuelsson, B., Dahlen, S. E., Lindgren, J. A., Rouzer, C. A., and Serhan, C. N. (1987) Leukotrienes and Lipoxins: Structures, Biosynthesis, and Biological Effects. *Science 237*, 1171−1176.

(21) Kuhn, H., Wiesner, R., Alder, L., Fitzsimmons, B. J., Rokach, J., and Brash, A. R. (1987) Formation of lipoxin B by the pure reticulocyte lipoxygenase via sequential oxygenation of the substrate. *Eur. J. Biochem. 169*, 593−601.

(22) Kuhn, H., Wiesner, R., Alder, L., Schewe, T., and Stender, H. (1986) Formation of lipoxin B by the pure reticulocyte lipoxygenase. *FEBS Lett. 208*, 248−252.

(23) Wecksler, A. T., Kenyon, V., Deschamps, J. D., and Holman, T. R. (2008) Substrate specificity changes for human reticulocyte and epithelial 15-lipoxygenases reveal allosteric product regulation. *Biochemistry 47*, 7364−7375.

(24) Wecksler, A. T., Kenyon, V., Garcia, N. K., Deschamps, J. D., van der Donk, W. A., and Holman, T. R. (2009) Kinetic and structural investigations of the allosteric site in human epithelial 15-lipoxygenase-2. *Biochemistry 48*, 8721−8730.

(25) Tsai, C. J., del Sol, A., and Nussinov, R. (2008) Allostery: Absence of a change in shape does not imply that allostery is not at play. *J. Mol. Biol. 378*, 1−11.

(26) Sola-Penna, M., Da Silva, D., Coelho, W. S., Marinho-Carvalho, M. M., and Zancan, P. (2010) Regulation of mammalian muscle type 6-phosphofructo-1-kinase and its implication for the control of the metabolism. *IUBMB Life 62*, 791−796.

(27) Sols, A. (1981) Multimodulation of enzyme activity. *Curr. Top. Cell. Regul. 19*, 77−101.

(28) Strater, N., Marek, S., Kuettner, E. B., Kloos, M., Keim, A., Bruser, A., Kirchberger, J., and Schoneberg, T. (2011) Molecular architecture and structural basis of allosteric regulation of eukaryotic phosphofructokinases. *FASEB J. 25*, 89−98.

(29) Nordlund, P., and Reichard, P. (2006) Ribonucleotide reductases. *Annu. Rev. Biochem. 75*, 681−706.

(30) Kolberg, M., Strand, K. R., Graff, P., and Andersson, K. K. (2004) Structure, function, and mechanism of ribonucleotide reductases. *Biochim. Biophys. Acta 1699*, 1−34.

(31) Reichard, P. (2002) Ribonucleotide reductases: The evolution of allosteric regulation. *Arch. Biochem. Biophys. 397*, 149−155.

(32) Ochi, K., Yoshimoto, T., Yamamoto, S., Taniguchi, K., and Miyamoto, T. (1983) Arachidonate 5-lipoxygenase of guinea pig peritoneal polymorphonuclear leukocytes. Activation by adenosine 5′-triphosphate. *J. Biol. Chem. 258*, 5754−5758.

(33) Furukawa, M., Yoshimoto, T., Ochi, K., and Yamamoto, S. (1984) Studies on arachidonate 5-lipoxygenase of rat basophilic leukemia cells. *Biochim. Biophys. Acta 795*, 458−465.

(34) Rouzer, C. A., and Samuelsson, B. (1985) On the nature of the 5-lipoxygenase reaction in human leukocytes: Enzyme purification and requirement for multiple stimulatory factors. *Proc. Natl. Acad. Sci. U.S.A. 82*, 6040−6044.

(35) Aharony, D., and Stein, R. L. (1986) Kinetic mechanism of guinea pig neutrophil 5-lipoxygenase. *J. Biol. Chem. 261*, 11512−11519.

(36) Mogul, R., Johansen, E., and Holman, T. R. (2000) Oleyl sulfate reveals allosteric inhibition of soybean lipoxygenase-1 and human 15-lipoxygenase. *Biochemistry 39*, 4801−4807.

(37) Aleem, A. M., Jankun, J., Dignam, J. D., Walther, M., Kuhn, H., Svergun, D. I., and Skrzypczak-Jankun, E. (2008) Human platelet 12-lipoxygenase, new findings about its activity, membrane binding and low-resolution structure. *J. Mol. Biol. 376*, 193−209.

(38) Dainese, E., Angelucci, C. B., Sabatucci, A., De Filippis, V., Mei, G., and Maccarrone, M. (2010) A novel role for iron in modulating the activity and membrane-binding ability of a trimmed soybean lipoxygenase-1. *FASEB J. 24*, 1725−1736.

(39) Di Venere, A., Salucci, M. L., van Zadelhoff, G., Veldink, G., Mei, G., Rosato, N., Finazzi-Agro, A., and Maccarrone, M. (2003) Structure-to-function relationship of mini-lipoxygenase, a 60-kDa fragment of soybean lipoxygenase-1 with lower stability but higher enzymatic activity. *J. Biol. Chem. 278*, 18281−18288.

(40) Blommel, P. G., and Fox, B. G. (2007) A combined approach to improving large-scale production of tobacco etch virus protease. *Protein Expression Purif. 55*, 53−68.

(41) Holman, T. R., Zhou, J., and Solomon, E. I. (1998) Spectroscopic and functional characterization of a ligand coordination mutant of soybean lipoxygenase-1: First coordination sphere analogue of human 15-lipoxygenase. *J. Am. Chem. Soc. 120*, 12564−12572.

(42) Jeon, W. B., Aceti, D. J., Bingman, C. A., Vojtik, F. C., Olson, A. C., Ellefson, J. M., McCombs, J. E., Sreenath, H. K., Blommel, P. G., Seder, K. D., Burns, B. T., Geetha, H. V., Harms, A. C., Sabat, G., Sussman, M. R., Fox, B. G., and Phillips, G. N., Jr. (2005) High-throughput purification and quality assurance of *Arabidopsis thaliana* proteins for eukaryotic structural genomics. *J. Struct. Funct. Genomics 6*, 143−147.

(43) Deschamps, J. D., Kenyon, V. A., and Holman, T. R. (2006) Baicalein is a potent in vitro inhibitor against both reticulocyte 15-human and platelet 12-human lipoxygenases. *Bioorg. Med. Chem. 14*, 4295−4301.

(44) Wecksler, A. T., Jacquot, C., van der Donk, W. A., and Holman, T. R. (2009) Mechanistic Investigations of Human Reticulocyte 15- and Platelet 12-Lipoxygenases with Arachidonic Acid. *Biochemistry 48*, 6259−6267.

(45) McAuley, W. J., Jones, D. S., and Kett, V. L. (2009) Characterisation of the interaction of lactate dehydrogenase with Tween-20 using isothermal titration calorimetry, interfacial rheometry and surface tension measurements. *J. Pharm. Sci. 98*, 2659−2669.

(46) Wecksler, A. T., Deschamps, J. D., Kenyon, V., Garcia, N. K., van der Donk, W. A., and Holman, T. R. (2009) Kinetic and structural investigations of the allosteric site in human epithelial 15-lipoxygenase-2. *Biochemistry 48*, 8721−8730.

(47) Reinhart, G. D. (2004) Quantitative analysis and interpretation of allosteric behavior. *Methods Enzymol. 380*, 187−203.

(48) Shang, W., Ivanov, I., Svergun, D. I., Borbulevych, O. Y., Aleem, A. M., Stehling, S., Jankun, J., Kuhn, H., and Skrzypczak-Jankun, E. (2011) Probing dimerization and structural flexibility of mammalian lipoxygenases by small-angle X-ray scattering. *J. Mol. Biol. 409*, 654−668.

(49) Ivanov, I., Shang, W., Toledo, L., Masgrau, L., Svergun, D. I., Stehling, S., Gómez, H., Di Venere, A., Mei, G., Lluch, J. M., Skrzypczak-Jankun, E., González-Lafont, À., and Kühn, H. (2012) Ligand-induced formation of transient dimers of mammalian 12/15-lipoxygenase: A key to allosteric behavior of this class of enzymes? *Proteins: Struct., Funct., Bioinf. 80*, 703−712.

(50) Maler, L., Blankenship, J., Rance, M., and Chazin, W. J. (2000) Site-site communication in the EF-hand Ca^{2+}-binding protein calbindin D9k. *Nat. Struct. Biol. 7*, 245−250.

(51) Yuan, C., Rieke, C. J., Rimon, G., Wingerd, B. A., and Smith, W. L. (2006) Partnering between monomers of cyclooxygenase-2 homodimers. *Proc. Natl. Acad. Sci. U.S.A. 103*, 6142−6147.